

Scripta-Ingenia

The quadrangular non-planar faces of Christchurch transitional cathedral



*Christchurch Cathedral, in 2006
(en.wikipedia.org)*



Shortly after the earthquake, 22 February 2011 (www.newshub.co.nz)



*Christchurch Cathedral in 2016
(Editor's personal photo)*

The beautiful city of Christchurch, in New Zealand, has been hit by several earthquakes over the last few years, with a most severe one in February 2011. The main cathedral was partially destroyed on that occasion and there was no consensual decision on what to do next. On the one hand there is the argument that it is better to demolish the remaining of the cathedral and build a new one on the same place, with modern architecture, and better suited to withstand strong earthquake impacts, this is clearly the logical and cheapest solution. On the other hand, there is a current of train of thought which defends the preservation of the original architecture of the cathedral. This alternative implies that the old cathedral has to be rebuilt and reinforced, while keeping its original and historical aspect. Clearly, this solution involves a greater amount of effort, financial and logistic. To the eyes of an European citizen, it would be odd to use an argument that an historical building only 150 years old has to be preserved at any cost, but one must not forget that from a kiwi's perspective (kiwi is how New Zealanders like to call themselves) this is utterly important due to the comparative low number of historical buildings in the country and that New Zealand's oldest European style building are under 200 years old.

In the meantime, the Archbishop of Canterbury (the administrative region of New Zealand to which Christchurch city belongs) needed a place to perform his sermons, while his followers needed a place to pray.

The solution developed by Japanese architect Shigeru Ban, who has proposed an innovative concept for a cathedral, is only meant to last for one or two decades; which is the time that would take to decide on the future of the old cathedral and then to either rebuild, or construct a new one.

One of the many interesting characteristics of the cardboard cathedral, as it is also called, is the fact that it has triangular back and front faces, both with the same height but different width. This creates a non-planar quadrangular faces on both sides, as it is visible in the picture on the next page.

A decision is to be taken until September this year on what will be the future of the cathedral.

A Scripta-Ingenia assume-se como uma revista de divulgação científica tratando temas da ciência e da tecnologia, cobrindo todas as áreas do saber no domínio das ciências exactas ou aplicadas. Interessa-se ainda por artigos de opinião, sobre tópicos científicos ou não, desde que escritos por autores na área das ciências e da engenharia, e que reflitam as suas opiniões enquanto membros dessa comunidade. Este é o seu número sete e corresponde ao Solstício de Inverno do ano de 2016.

Director and Chief Editor — Nelson Martins-Ferreira
CDRSP-ESTG, IPEiria



The transitional cardboard cathedral in Christchurch, New Zealand. In the picture we can observe the non-planarity of the lateral face due to the difference of width between the front and back triangular faces.
<http://www.addingtonbrass.com/wp-content/uploads/2015/06/Christchurch-Cathedral.jpg>

Electro-Magnetic Space-Time Duality for 2+1-Dimensional Stationary Classical Solutions

by P. CASTELO FERREIRA

Centre for Rapid and Sustainable Product Development
Polytechnic Institute of Leiria
Author email: pedro.castelo.ferreira@gmail.com

Abstract In this paper it is studied a space-time duality web that maps electric into magnetic (and magnetic into electric) charged classical stationary rotating solutions for 2+1-dimensional Abelian Einstein Maxwell Chern-Simons theories. A first duality map originally suggested by Kogan for static charged solutions is extended to stationary rotating space-times and are suggested two new space-time dualities maps. The three dualities complete a close duality web. It is also shown that in 3+1-dimensions these dualities are only possible for systems which exhibit non-projected cylindrical symmetry and are not related to the standard electromagnetic duality of Maxwell equations which acts on the physical fields and charges. Generalization to N -form theories in higher dimensional space-times is briefly discussed.

1 Introduction

In an attempt to justify the quantization of electric charge e Dirac concluded that magnetic charge g should also exist in nature and it is consistently predicted from the quantum theory solutions [1]. Although magnetic monopoles have never been detected experimentally this theoretical observation is still today the best justification for the experimentally observed quantization of electric charge. Following Dirac argument a generalization of the standard Maxwell electromagnetism explicitly including magnetic charges is straight forward achievable by considering both electric 4-currents $J_e = (\rho_e, \mathbf{j}_e)$ and magnetic 4-currents $J_g = (\rho_g, \mathbf{j}_g)$, where the ρ 's are the charge densities and the \mathbf{j} 's are the current densities. In particular was noticed that the covariant 3+1-dimensional Maxwell equations, with both electric and magnetic currents, are invariant under the following rotation of the electromagnetic fields $\mathbf{E} + i\mathbf{B} \leftrightarrow e^{i\phi}(\mathbf{E} + i\mathbf{B})$ and $J_e + iJ_g \leftrightarrow e^{i\phi}(J_e + iJ_g)$, where \mathbf{E} is the electric field and \mathbf{B} is the magnetic field (in this paper are employing natural units $\hbar = c = 1$). This field map is generally known as the electromagnetic duality (see [2, 3] for a review in the subject).

The electromagnetic duality was further explored in the context of 3+1-dimensional charged gravitational solutions, namely in the works of Deser and al. [4, 5] this field duality is applied to black hole solutions in several dimensions, such that computed electric solutions are mapped into dual magnetic solutions. Also in 2+1-dimensional (planar) systems exact field and gravitational electric and magnetic charged solutions have been extensively studied in the literature [6, 7, 8, 9, 10, 12, 11, 13, 14] (see also references therein). The motivation for these works is not purely theoretical as 2+1-dimensional systems effectively describe real physical phenomena in

condensed matter systems [15] and experimental searches for both elementary magnetic monopoles as well as for extended magnetically charged solutions in 3+1- and 2+1-dimensional systems are justified by the original Dirac argument [16].

For planar systems, a duality between electric and magnetic charged solutions was suggested by Kogan [6, 7]. This duality acts directly in the 2+1-dimensional space-time manifold ($t \rightarrow i\varphi$ and $\varphi \rightarrow it$) instead of acting in the electromagnetic fields and was applied to Abelian Einstein Maxwell Chern-Simons theories for static radial symmetric metrics. In this paper this map is extended to stationary rotating spaces and a new distinct space-time duality map is suggested ($t \rightarrow \varphi$ and $\varphi \rightarrow t$) that also maps electric into magnetic solutions (and magnetic into electric solutions). These two duality maps will further be related through a third duality map consisting of a double Wick rotation ($t \rightarrow it$ and $\varphi \rightarrow i\varphi$) such that a close duality web is obtained. The third duality does not map electric into magnetic solutions, instead maps standard gauge fields into ghost fields by swapping the relative sign between the gravitational and gauge sector of the theory. The lifting of these duality maps to 3+1-dimensional space-time as well as their possible application to N -form theories in higher dimensional space-times [17] is briefly discussed.

In section 2 the original duality map as suggested by Kogan is reviewed and generalized to stationary rotating space-times. In section 3 a new duality map is suggested and in section 4 both dualities are related through a third duality map which is a double Wick rotation such that a close duality web is obtained. In section 5 the dualities are generalized to non-projected four dimensional solutions with cylindrical symmetry and their application to N -form theories in higher dimensional space-times is briefly discussed.

2 Original Duality for 2 + 1-Dimensional Rotating Space-Times

The action for Abelian Einstein Maxwell Chern-Simons theory in a 2 + 1-dimensional Minkowski space-time manifold M is

$$S = \int_M \left(\tilde{R} * 1 - \tilde{F} \wedge * \tilde{F} + m \tilde{A} \wedge \tilde{F} \right), \quad (1)$$

where $\tilde{R} * 1$ is the Einstein term (Ricci scalar), $\tilde{F} = d\tilde{A}$ is the Maxwell tensor such that $\tilde{F} \wedge * \tilde{F}$ is the Maxwell term, $m \tilde{A} \wedge \tilde{F}$ is the topological Chern-Simons term and m is the topological mass of the gauge field \tilde{A} which is physically interpreted as the gauge photon field in planar systems. We briefly recall that in 2 + 1-dimensional Maxwell theory the topological Chern-Simons term arises as a quantum correction and has the effect of generating a mass m to the photon field \tilde{A} [18]. Hence for consistence of the theory the Chern-Simons should be considered in the theory and does not depend explicitly on the geometry of the manifold, instead is coupled by the equations of motion for the gauge field \tilde{A} to the Maxwell term, which in turn couples to the gravitational sector. Generally these theories are also known as topologically massive gauge theories. It is also relevant to further note that to avoid the gauge field being interpreted as a tachyon (having classical imaginary mass) the Maxwell and Chern-Simons term must have opposite sign (for $m > 0$) [11]. As for the relative sign between the Einstein term and the Maxwell term imposes whether the gauge field \tilde{A} is interpreted as a standard gauge field (opposite sign) or a ghost field (same sign). Specifically for standard gauge fields the quantum states have positive energy eigenvalues while for ghost fields have negative energy eigenstates (see [19] and references therein for a discussion of relative sign choices and derivation of Hamiltonian quantization in 2 + 1- and 3 + 1-dimensional embeddings).

The original duality map consist in mapping electric into magnetic solutions (as well as magnetic into electric solutions) by exchanging the role of the time coordinate t and the angular coordinate φ [6]

$$\begin{aligned} t &\rightarrow i\varphi, \\ \varphi &\rightarrow it. \end{aligned} \quad (2)$$

With the objective of generalizing this duality map to stationary rotating space-times let us consider a 2 + 1-dimensional metric on the ADM form [20]

$$ds^2 = -\tilde{f}^2 dt^2 + dr^2 + \tilde{h}^2 (d\varphi + \tilde{N} dt)^2, \quad (3)$$

and the standard electric and magnetic field definitions

$$\begin{aligned} \tilde{E} &= \tilde{F}_{tr}, \\ \tilde{B} &= \tilde{F}_{r\varphi}, \end{aligned} \quad (4)$$

where we recall that in planar systems the magnetic field \tilde{B} is a scalar while the electric field \tilde{E} is a 2-vector. Let us further introduce a Cartan triad for the metric (3) $e^0 = f dt$ and $e^2 = h(d\varphi + Adt)$ (see [21]). Then the duality map (2) is simply interpreted as the duality map for the triad elements $e^0 \leftrightarrow e^2$ (see [13]). With respect to the several gravitational fields this accounts for the following field maps

$$\begin{aligned} \tilde{f} &\rightarrow ih, \\ \tilde{h} &\rightarrow if, \\ \tilde{E} &\rightarrow -iB, \\ \tilde{B} &\rightarrow -iE, \end{aligned} \quad (5)$$

such that the following dual metric parameterization is

$$ds_{\text{dual}}^2 = -f^2 (dt + Nd\varphi)^2 + dr^2 + h^2 d\varphi^2. \quad (6)$$

As for the gauge sector the Maxwell and Chern-Simons terms transform as $-\tilde{F} \wedge * \tilde{F} + m \tilde{A} \wedge \tilde{F} \rightarrow +F \wedge * F - mA \wedge F$. Hence the gauge sector swaps the relative sign with respect to the gravitational sector such that standard gauge fields are mapped into ghost gauge fields.

The tensor components of the two metrics corresponding to ds^2 and ds_{dual}^2 are

$$\left\{ \begin{array}{l} \tilde{g}_{00} = -\tilde{f}^2 + \tilde{h}^2 \tilde{N}^2 \\ \tilde{g}_{11} = 1 \\ \tilde{g}_{22} = \tilde{h}^2 \\ \tilde{g}_{02} = \tilde{h}^2 \tilde{N} \end{array} \right\}, \quad \left\{ \begin{array}{l} g_{00} = -f^2 \\ g_{11} = 1 \\ g_{22} = h^2 - f^2 N^2 \\ g_{02} = -f^2 N \end{array} \right\}, \quad (7)$$

such that these two parameterizations are straight forward related by the following equalities

$$\begin{aligned} \tilde{f}^2 &= \frac{f^2 h^2}{h^2 - f^2 N^2}, \\ \tilde{h}^2 &= h^2 - f^2 N^2, \\ \tilde{N} &= -\frac{N f^2}{h^2 - f^2 N^2}. \end{aligned} \quad (8)$$

As for the ADM metric signature behavior for each specific solution, under the duality maps, are obtained the following cases

$$\begin{aligned} h^2 - f^2 N^2 > 0 &\Rightarrow \text{duality maintains signature,} \\ h^2 - f^2 N^2 < 0 &\Rightarrow \text{duality changes signature.} \end{aligned} \quad (9)$$

This is directly concluded by inspection of the equalities (8) such that the duality map (2) only maintains the metric signature for regions of space-time where the solutions obey the constraint $h^2 - f^2 N^2 > 0$. This feature

only arises for rotating space-times, in the limit $N \rightarrow 0$ the constraint becomes $h^2 > 0$ (which is verified as long as h is real) such that the metric always maintains the signature under this duality.

It is relevant to stress once more that the duality (2) is a map of the space-time coordinates, although the electromagnetic fields transform accordingly (5) this is not a duality map of the electromagnetic fields. Also, by swapping the relative sign between the gravitational and gauge terms, it has the effect of mapping standard gauge fields into ghost fields.

Next we will show that this duality map is not the only possible duality.

3 Another Possible Duality for Rotating Space-Times

Generally, for a given particular solution already computed, it may be desired to obtain the opposite sign transformation properties for the metric signature to the one expressed by inequalities (9). Hence it is straight forward to conclude that a possible duality map is to consider a direct swapping of the time and angular coordinates without the imaginary phase

$$\begin{aligned} t &\rightarrow \varphi, \\ \varphi &\rightarrow t. \end{aligned} \quad (1)$$

With respect to the several fields this accounts for the following field map

$$\begin{aligned} \tilde{f} &\rightarrow \hat{h}, \\ \tilde{h} &\rightarrow \hat{f}, \\ \tilde{E} &\rightarrow -\hat{B}, \\ \tilde{B} &\rightarrow -\hat{E}, \end{aligned} \quad (2)$$

where hatted fields are employed to distinguish between the two dualities given in (2) and (1). The dual metric parameterization is straight forwardly written as

$$d\hat{s}_{\text{dual}}^2 = \hat{f}^2(dt + \hat{N}d\varphi)^2 + dr^2 - \hat{h}^2d\varphi^2, \quad (3)$$

and the gauge sector maintains its relative sign with respect to the gravitational sector as the Maxwell and Chern-Simons terms transform as $-\tilde{F} \wedge * \tilde{F} + m\tilde{A} \wedge \tilde{F} \rightarrow -\hat{F} \wedge * \hat{F} + m\hat{A} \wedge \hat{F}$ such that standard gauge fields are mapped into standard gauge fields.

The tensor components of the dual metric (3) are

$$\begin{cases} \hat{g}_{00} = \hat{f}^2 \\ \hat{g}_{11} = 1 \\ \hat{g}_{22} = -\hat{h}^2 + \hat{f}^2 \hat{N}^2 \\ \hat{g}_{02} = \hat{f}^2 \hat{N}. \end{cases} \quad (4)$$

We can relate these two parameterization by the following equality

$$\begin{aligned} \tilde{f}^2 &= \frac{\hat{f}^2 \hat{h}^2}{-\hat{h}^2 + \hat{f}^2 \hat{N}^2} \\ \tilde{h}^2 &= -\hat{h}^2 + \hat{f}^2 \hat{N}^2 \\ \tilde{N} &= -\frac{\hat{N} \hat{f}^2}{-\hat{h}^2 + \hat{f}^2 \hat{N}^2} \end{aligned} \quad (5)$$

As for the behavior of the metric signature under the above map, by inspection of the equalities (5), we obtain the following cases:

$$\begin{aligned} -\hat{h}^2 + \hat{f}^2 \hat{N}^2 > 0 &\Rightarrow \text{duality maintains signature,} \\ -\hat{h}^2 + \hat{f}^2 \hat{N}^2 < 0 &\Rightarrow \text{duality changes signature,} \end{aligned} \quad (6)$$

hence with the opposite sign of inequalities (9).

Hence, for a given solution, both the metric signature and the relative sign between the gravitational and gauge sector are mapped distinctly under the duality maps (2) and (1).

4 Double Wick Rotation as a Duality

Let us note that both dualities as given by (2) and (1) are straight forwardly related by a double Wick rotation map

$$\begin{aligned} t &\rightarrow it \\ \varphi &\rightarrow i\varphi \end{aligned} \quad (7)$$

for which the fields map accordingly has

$$\begin{aligned} f &\rightarrow if \\ h &\rightarrow ih \\ E &\rightarrow iE \\ B &\rightarrow iB \end{aligned} \quad (8)$$

such that the factor $-h^2 + f^2 N^2 \rightarrow \hat{h}^2 - \hat{f}^2 \hat{N}^2$ swaps sign and the the gauge sector changes its relative sign with respect to the gravitational sector $+F \wedge *F - mA \wedge F \rightarrow -\hat{F} \wedge * \hat{F} + m\hat{A} \wedge \hat{F}$. Hence gauge fields are mapped into ghost gauge fields.

In this way from a given electric or magnetic solution for the metric parameterization (3) one can find a magnetic or electric solution (respectively) employing the above duality maps (2) and (1). The choice of the duality to be employed depends on the specific form of the solutions such that the dual metric signature is set accordingly either by condition (9) or (6) and whether the

gauge fields are intended to be ghost fields or standard fields. Also by employing (7) one can, from a given charged solution, obtain another charged solution of the same kind with the opposite ADM metric signature and distinct gauge field interpretation (for standard fields are obtained ghost fields and for ghost fields are obtained standard fields). This web of dualities is pictured in figure 4.

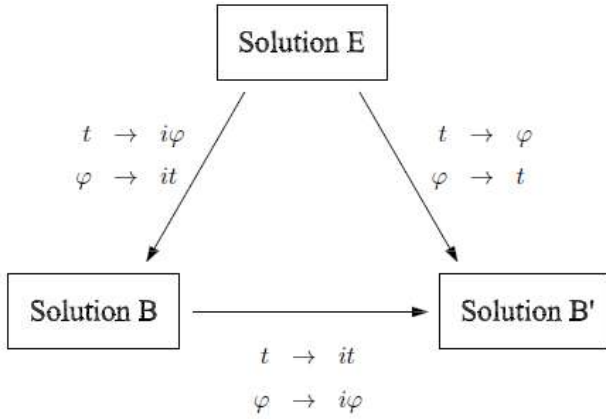


Figure 1: Web of Dualities. The dualities can be considered in both directions. In the picture are expressed only the dualities for the directions of the arrows.

For last let us note that, as expected from covariance, for all the three dualities the Einstein term in the action (1) does not change sign as it is explicitly written in powers of 4 with respect to the metric fields f 's and h 's ($i^4 = +1$). However this fact does not imply that it is constant across space-time, generally and as expected it changes across space-time for each particular solution depending on the matter distribution.

5 Dualities in 3 + 1D and Higher Dimensional Space-Times

In 2 + 1-dimensions the magnetic field is a scalar (corresponding to $\tilde{B}_{(3D)} = \tilde{F}_{r\varphi}$) and planar system can be interpreted either as a projected 3 + 1-dimensional system or as embedded systems [19]. So far the dualities (2), (1) and (7) apply to both these frameworks and implicitly the angular component of the electric field is necessarily null, $\tilde{E}_{(3D)}^\varphi = \tilde{F}^{0\varphi} = 0$. This result is imposed by the Einstein equations (gravitational equation of motion) as the radial shift function in the metric [13] does not constitute a physical gravitational degree of freedom in 2 + 1-dimensional gravity [21].

More generally in a full 3 + 1-dimensional one can assume non-projected cylindrical symmetry around the θ direction such that the projected magnetic field corresponds indeed to the θ component of the non-projected

magnetic field, $\tilde{B}_{(3D)} = \tilde{B}_{(4D)}^\theta$ and $\tilde{E}_{(4D)}^\varphi = 0$. Concerning the projection of four dimensional gravity to three dimensional space-times we refer the reader to [8, 9].

Then for 3 + 1-dimensional solutions with cylindrical symmetry we obtain two possible components for the electric and magnetic field

$$\begin{cases} \tilde{E}_{(4D)}^r = \tilde{F}^{0r} \\ \tilde{E}_{(4D)}^\theta = \tilde{F}^{0\theta} \end{cases}, \begin{cases} \tilde{B}_{(4D)}^r = \tilde{F}_{\varphi\theta} \\ \tilde{B}_{(4D)}^\theta = \tilde{F}_{r\varphi} \end{cases}, \quad (1)$$

such that the dualities discussed so far map the radial and polar electric fields into the polar and radial magnetic fields, respectively. The first field map (5) is equivalent to the field map

$$\begin{aligned} \tilde{E}_{(4D)}^r &\rightarrow -iB_{(4D)}^\theta, \\ \tilde{E}_{(4D)}^\theta &\rightarrow -iB_{(4D)}^r, \\ \tilde{B}_{(4D)}^r &\rightarrow -iE_{(4D)}^\theta, \\ \tilde{B}_{(4D)}^\theta &\rightarrow -iE_{(4D)}^r, \end{aligned} \quad (2)$$

and the second field map (2) is equivalent to the field map

$$\begin{aligned} \tilde{E}_{(4D)}^r &\rightarrow -\hat{B}_{(4D)}^\theta, \\ \tilde{E}_{(4D)}^\theta &\rightarrow -\hat{B}_{(4D)}^r, \\ \tilde{B}_{(4D)}^r &\rightarrow -\hat{E}_{(4D)}^\theta, \\ \tilde{B}_{(4D)}^\theta &\rightarrow -\hat{E}_{(4D)}^r. \end{aligned} \quad (3)$$

In this way the dualities are lifted from a 2 + 1-dimensional system to a 3 + 1-dimensional system with cylindrical symmetry. As expected it is not possible to generalize the dualities for generic stationary solutions to generic 3 + 1-dimensional system that do not possess cylindrical symmetry. In order to conclude it, it is enough to consider the remaining field components $\tilde{E}_{(4D)}^\varphi = \tilde{F}^{0\varphi}$ and $\tilde{B}_{(4D)}^\varphi = -\tilde{F}_{r\theta}$ which are maintained (up to sign changes) by the field maps (5) and (2).

It is interesting to note that a generalization is possible for N -form theories in higher dimensional space-times [5]. For instance in 5 + 1-dimensions, by considering the 2-form fields $E^{IJ} = F^{0IJ}$ and $B^{IJ} = \epsilon^{IJKLM} F_{KLM}/6$, under the duality ($t \rightarrow ix^5$, $x^5 \rightarrow it$) we obtain the map $E^{12} \leftrightarrow -iB^{34}$, $E^{13} \leftrightarrow -iB^{24}$, $E^{14} \leftrightarrow -iB^{23}$, $E^{23} \leftrightarrow -iB^{14}$, $E^{24} \leftrightarrow -iB^{13}$ and $E^{34} \leftrightarrow -iB^{12}$.

We recall once more that there is no relation of these dualities with the usual electromagnetic duality of the gauge fields [2, 3, 4, 5]. The original electromagnetic duality rotates the same components of the electric and magnetic into each other not mapping the space-time components of the fields as opposed to the dualities just discussed.

6 Conclusions

In this paper was developed a space-time duality web that allows to map electric into magnetic classical solutions into each other. These dualities may generally change the ADM metric signature as given in (3). Then, given that the coefficient of dr^2 is positive (see [13] for a discussion on different choices of signatures), the original Minkowski signature is considered to be the one that holds the coefficient of dt^2 negative and the coefficient of $d\varphi^2$ positive, this means that we are aiming at solutions with $\tilde{f}^2 > 0$ and $\tilde{h}^2 > 0$. Also from the explicit form of the three possible field maps (5), (2) and (8) one may map real solutions into imaginary solutions. Nevertheless by imposing reality conditions and properly constraining the parameters and variables of the original solutions it is generally possible to achieve real solutions.

Also the mapping of the relative sign between the gravitational sector and the gauge sector was analysed such that duality (2) and (7) maps standard gauge fields and ghost gauge fields into each other while duality (1) does not.

We resume the results obtained in the next table.

duality	maintains signature	standard \leftrightarrow ghost
$t \rightarrow i\varphi$ $\varphi \rightarrow it$	$h^2 - f^2 N^2 > 0$	yes
$t \rightarrow \varphi$ $\varphi \rightarrow t$	$h^2 - f^2 N^2 < 0$	no
$t \rightarrow it$ $\varphi \rightarrow i\varphi$	no	yes

It is also explicitly concluded that the dualities studied are not related to the electromagnetic duality of the electromagnetic fields and, although valid for four dimensional solutions with cylindrical symmetry, cannot be generalized to generic solutions on 3+1-dimensional systems. However we give an example in six dimensional space-time that show that the dualities can be generalized to N-form theories in higher dimensional space-times.

Acknowledgements This work was supported by SFRH/BPD/17683/2004 up to 2007 and by CENTRO-01-0145-FEDER-000014 from 2017 onward.

Referências

- [1] P. A. M. Dirac, *Quantized Singularities in the Electromagnetic Field*, Proc.Roy.Soc.Lond. **A133** (1931) 60-72; *The Theory of magnetic poles*, Phys.Rev. **74** (1948) 817-830.
- [2] J. D. Jackson, *Classical Electrodynamics*, 2nd Edition, John Wiley & Sons, 1975 (see pp 273).

- [3] D. I. Olive, *Exact Electromagnetic Duality*, Nucl. Phys. Proc. Suppl. **45A** (1996) 88-102; Nucl. Phys. Proc. Suppl. **46** (1996) 1-15, hep-th/9508089
- [4] S. Deser, M. Henneaux and C. Teitelboim, *Electric-Magnetic Black Hole Duality*, Phys. Rev. **D55** (1997) 826-828, hep-th/9607182; S. Deser *Black Hole Electromagnetic Duality*, AIP Conf. Proc. **400** (1997) 437, hep-th/9701157.
- [5] S. Deser, A. Gomberoff, M. Henneaux and C. Teitelboim, *Duality, Self-Duality, Sources and Charge Quantization in Abelian N-Form Theories*, Phys. Lett. **B400** (1997) 80-86, hep-th/9702184.
- [6] I. I. Kogan, *About Some Exact Solutions for 2 + 1 Gravity Coupled to Gauge Fields*, Mod. Phys. Lett. **A7** (1992) 2341-2350, hep-th/9205095.
- [7] I. I. Kogan, *Black Hole Spectrum, Horizon Quantization and All That: (2+1)-dimensional example*, hep-th/9412232.
- [8] S. Chandrasekhar, *Cylindrical Waves in General Relativity*, Proc. Roy. Soc. Lond. **A408** (1986) 209-232
- [9] J. P. S. Lemos, *Cylindrical Black Hole in General Relativity*, Phys. Lett. **B353** (1995) 46-51, gr-qc/9404041.
- [10] P. C. Stichel, *Deformed Chern-Simons interaction for nonrelativistic point particles*, Phys. Lett. **B526** (2002) 399-404, arXiv:hep-th/0112025.
- [11] S. Deser and B. Tekin, *Massive, topologically massive, models*, Class. Quant. Grav. **19** (2002) 97-100, hep-th/0203273.
- [12] A Ferstl, B. Tekin and V. Weir, *Gravitating Instantons in Three-Dimensional Anti-De Sitter Space*, Phys. Rev. **D62** (2000) 064003, hep-th/0002019; S. Deser and B. Tekin, *Energy in Topologically Massive Gravity*, Class. Quant. Grav. **20** (2003) L259, gr-qc/0307073; C. Nazaroğlu, Y. Nutku, B. Tekin, *Covariant Symplectic Structure and Conserved Charges of Topologically Massive Gravity*, Phys. Rev. **D 83** (2011) 124039, arXiv:1104.3404.
- [13] P. Castelo Ferreira, *Rotating Electric Classical Solutions of 2 + 1 D U(1) Einstein Maxwell Chern-Simons*, Class.Quant.Grav. **23** (2006) 3679-3706 hep-th/0506244.
- [14] O. J. C. Dias, *Black Hole Solutions and Pair Creation of Black Holes in Three, Four and Higher Dimensional Spacetimes*, PhD Thesis (2004), arXiv:hep-th/0410294.
- [15] T. Ando, *Theory of Quantum Transport in a Two-Dimensional Electron System under Magnetic Fields. III. Many-Site Approximation*, J. Phys. Soc. Jpn. **37**

- (1974) 622-630; K. von Klitzing, G. Dorda and M. Pepper, *New method for high accuracy determination of the fine structure constant based on quantized Hall resistance*, Phys. Rev. Lett. **45** (1980) 494-497; R. B. Laughlin, *Quantized Hall conductivity in two-dimensions*, Phys. Rev. **B23** (1981) 5632-5733; F. Wilczek, *Magnetic Flux, Angular Momentum, and Statistics*, Phys. Rev. Lett. **48** (1982) 1144-1146; *Quantum Mechanics of Fractional Spin Particles*, Phys.Rev.Lett. **49** (1982) 957-959.
- [16] S. Balestra et al, *Magnetic Monopole Bibliography-II*, arXiv:1105.5587; D. E. Groom, *Magnetic Monopoles Searches* in Eidelman et al. (Particle Data Group), Phys. Lett. **B592** (2004) 1; D. Milstead and E. J. Weinberg, *Magnetic Monopoles* in C. Patrignani et al. (Particle Data Group), Chin. Phys. **C40** (2016) 100001; Milde et al, *Unwinding of a Skyrmion Lattice by Magnetic Monopoles*, Science **340** (2013) 6136:1076.
- [17] J. Kunz et al., *$D = 5$ Einstein-Maxwell-Chern-Simons black holes*, Phys.Rev.Lett. **96** (2006) 081101, hep-th/0510250; *A Note on Rotating Charged Black Holes in Einstein-Maxwell-Chern-Simons Theory*, Phys.Rev. **D74** (2006) 105004, hep-th/0607201; A. M. Ghezelbash, *Cosmological Solutions on Atiyah-Hitchin Space in Five Dimensional Einstein-Maxwell-Chern-Simons Theory*, Phys.Rev. **D81** (2010) 044027, arXiv:1001.5066; *Exact convoluted solutions in higher-dimensional Einstein-Maxwell theory*, Phys.Rev. **D90** (2014) 084047, arXiv:1409.3197; *Cosmological solutions in five dimensional Einstein-Maxwell-dilaton theory*, Phys.Rev. **D91** (2015) 084003, arXiv:1502.00951;
- A. M. Ghezelbash and V. Kumar, *Exact helicoidal and catenoidal solutions in five- and higher-dimensional Einstein-Maxwell theory*, Phys.Rev. **D95** (2017) 124045, arXiv:1704.01476; Z. Haghani, T. Harko and S. Shahidi, *The Maxwell-Chern-Simons gravity, and its cosmological implications*, Eur.Phys.J. **C77** (2017) 514, arXiv:1704.06539.
- [18] S. Deser, R. Jackiw and S. Templeton, *Topologically Massive Gauge Theories*, Annals Phys. **140** (1982) 372-411; Annals Phys. **281** (2000) 409-449; *Three-Dimensional Massive Gauge Theories*, Phys. Rev. Lett. **48** (1982) 975-978; A. J. Niemi and G. W. Semenoff, *Axial Anomaly Induced Fermion Fractionization and Effective Gauge Theory Actions in Odd Dimensional Space-Times*, Phys. Rev. Lett. **51** (1983) 2077; A. N. Redlich, *Parity Violation and Gauge Noninvariance of the Effective Gauge Field Action in Three Dimensions*, Phys. Rev. **D29** (1984) 2366-2374; S. R. Coleman and B. Hill, *No More Corrections to the Topological Mass Term in QED3*, Phys. Lett. **B159** (1985) 184-188.
- [19] P. Castelo Ferreira, *$U_e(1) \times U_g(1)$ actions in $2 + 1$ dimensions: Full vectorial electric and magnetic fields*, EPL **79** (2007) 20004, hep-th/0703193; *Canonical functional quantization of pseudo-photons in planar systems*, AIP Conf.Proc. **1023** (2008) 143-147, arXiv:0712.0710.
- [20] R. Arnowitt, S. Deser and C. W. Misner, *The Dynamics of General Relativity* (1962) 227-265.
- [21] S. Carlip, *Quantum Gravity in $2 + 1$ Dimensions*, Cambridge University Press.

Characterization of a Hospital Emergency Service Queue — A

Case Study

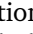
by MÁRIO CARVALHO^a, RUI SANTOS^{a,b}, AND LILIANA FERREIRA^{a,c}


^a School of Technology and Management, Polytechnic Institute of Leiria, Portugal

^b Center of Statistics and Applications of the University of Lisbon (CEAUL)

^c Center for Mathematics, Fundamental Applications and Operations Research (CMAFCIO)

Abstract

This research aims at emphasizing the potential of using simulation when studying the behavior of a hospital emergency queue. Further, it provides the characterization of the queuing system in a hospital emergency service. Thus, it was considered the emergency department queue of the Hospital de Santo André (HSA) located in Leiria – Portugal as a case study and it was modeled through simulation using the  software. The characterization was based on the hospital's dataset of 2014. The patient's data includes records since the arrival time at the hospital until the exit point. Other measures and characteristics that influence the time spent by the patient in the emergency service were considered. Simulation was applied in order to develop a suitable queue model for the case study. It was simulated a matrix with the patient's data that was compared with the real data provided by HSA. In this process, the priorities of patients defined by the Manchester triage system were also taken into consideration. Finally, the proposed simulation approach helps to address several different scenarios. The generated information is influential for the decision makers and provides insights about improvements that may occur in the efficiency of the HSA emergency service. The results of the proposed simulation model applied to the HSA's case study are discussed.

Keywords: Emergency service, Queuing models,  software, Simulation, Statistical distributions, Triage.

1 Introduction

Emergency services play an increasingly important role in the National Health Service, where waiting times are a key factor in the patient satisfaction [3, 7]. Emergency Services exist to provide patients a quick response to potential health hazards. An emergency is any situation in which a delayed diagnosis or treatment generates severe risks or injuries to the victim. Patients in a serious condition require a faster service compared to less severe situations, since a prolonged waiting time can compromise the patient's health. It is therefore required to apply some methodology for the classification of the patient's clinical priority, such as the Manchester Triage System [9]. After complete the registration in the emergency service, the patient is forwarded to a triage office and is submitted to a preliminary observation. Here, through the identification of some symptoms or signs, it is assigned a degree of clinical priority to the patient and thereby a recommended maximum waiting time until the first medical observation.

The main goal of the queue theory is to optimize the performance of a system in order to reduce their operating costs and to increase patient satisfaction [20]. The knowledge of some parameters in the study of waiting queues allows both determining which set of priority rules maximize the attendance rate and sizing the resources to control the waiting times. Some key information are the average time of patients arrivals, the waiting time for

receiving assistance, the number of patients simultaneously waiting to be served and the occupancy rate of each feature. The solution for such problems is usually found by looking through the simulation for the best setup of rules and the best resource dimension. Instead of looking directly to evaluate the performance of the emergency service, it can be simulated by using probability distributions, allowing random generation of multiple events that occur in the different integration units (admission, triage and appointment) [11].

Applying the simulation of waiting queues allows to analyse the typical behavior of emergency service's queues and, therefore, provides insights into instrumental variables that support management plans designed by decision makers [15, 29].

Queuing theory and its analysis has already been used in healthcare services. Its application can assist in reducing patient waiting times in an emergency service [1]. However, its use in this sector is still not embracing as it could be [8]. The reader is referred to [8, 21] for an introduction to the use of queuing, where several models are described and its characteristics and performance measures are presented.

The advantages of queuing analysis in healthcare services, covering topics such as policies for bed allocation, staffing or services improvements are highlighted by [10]. [20] presents queuing models as one of the possible quantitative techniques to analyze health care service capacity and performance. [18] uses a queuing

model to represent UK Accident and Emergency departments in order to analyze the Government's targets for serving the patients in those departments. A queue system model was developed by [5] to describe the complexity of an emergency cardiac service. Likewise, [14] employs queuing theory to estimate the average waiting time across patients and to analyze how the patient flow can help the designer or manager of a hospital make decisions on the allocation of resources in a hospital. A UK study [28] reviews the techniques that can be developed to analyze emergency service systems according to the demand, focusing on the optimization of shift schedules and scales. [24] uses a simulation model in order to identify how to make emergency services from 5 hospitals in Israel more efficient, and [6] proposes a simulation algorithmic (using empirical data from a hospital in Israel) to enable decision makers to optimally schedule evaluations for patients who are waiting for treatment in the emergency services, mainly in the triage process.

Queuing theory has also been used in some Portuguese research studies developed within hospital environments. [16] and [17] use simulation via Arena software in order to develop applications for specific case studies about Portuguese hospitals services. Nevertheless, they are not based on statistical distributions between the database and the simulation nor use the creation of various scenarios for system optimization. The study [26] developed an application that presents information about waiting times, makes the calling of patients and announces messages.

This paper refers to the data of the patients route, concerning the arrival time to the hospital's emergency services, the admission hour, the triage hour, the classification of the patient's triage, the doctor's appointment time, the departure time, as well as other steps and/or features that influence the time spent by the patient in the hospital's emergency services. Considering the number of servers, the statistical distribution of arrival times and waiting times, the queue discipline and the various stages of the system, an appropriate queue model was adopted for this case study. A matrix with the patient's data was generated through the simulation and the statistical distribution between this model and the real database were compared in order to identify whether the two datasets are characterized by the same distributions. Moreover, it sought to find the most suitable values for the simulation parameters in order to obtain a precise model, taking into account its comparison with the real database. An essential part of the simulation was the addition of the component of priorities through the Manchester triage system, which classifies the patients according to their urgency. This simulation allowed to build multiple scenarios and to obtain results for a deeper understanding of the system behavior regarding to efficiency of queues in the HSA emergency service. Therefore, it provides relevant information to examine possible efficiency improvements of the service.

This paper is organized as follows. In Section 2 a brief introduction to the queues theory and existing models is presented. Section 3 explains the applied methodology, with particular focus on the implemented features through software simulation. In section 4 various scenarios are created by changing values of the model parameters, thereby enabling to test the system efficiency. The model's stability is also tested and the results and the respective analyses are presented. Finally, in Section 5, the main conclusions are provided and both final thoughts and possible future work approaches are displayed.

2 The Waiting Queue System

A queuing model is basically a service system that directs a customer to one or more servers to be served [10]. If there is an available server, the client can be served immediately, but if all the servers are busy the client must wait in the line for the service. Figure 1 shows a basic system of queues with some of its main components: the customer arrival to the system, the queue and the server (who provides the service). The queue discipline, the system capacity, the number of servers and the number of stages that make up the system are also important characteristics of a queuing system [8].

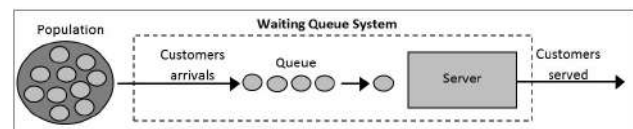


Fig. 1 — Basic representation of waiting queue system

Customers requiring a specific service arrive from a particular population and when entering in the waiting queuing system they join the queue. Each member of the queue is selected to be served in accordance with a rule called queue discipline. The requested service is executed by the server and then the customer leaves the queuing system.

Let “Customers Arrivals” and “Server Time” be two random variables. It is essential to study the statistical distribution that characterizes these variables. This is the starting point for the use of analytical models or simulation techniques to support queue management.

2.1 Manchester triage system

Triage is a system of priorities, applied (for example) in hospital emergency services. It aims at providing quick-services towards any risk situations for health. Whenever the clinical situation is severe, the patient should be immediately aided. In Manchester Triage there are five categories, represented by five colours (red, orange, yellow, green and blue), each one matching a degree of severity as well as an ideal (maximum) time within the patient must be treated (i.e., the target time). This correspondence is shown in Table 1. Thus, patients classified with

the highest priority by the triage system will be served before lower priority's patients. For example, if the patient is considered 'emergent' (red), the entrance to the assigned server should be immediate. If it is considered as 'very urgent' (orange) or 'urgent' (yellow), the patient will go to an internal waiting room and will wait to be seen and treated by a doctor. If it is classified as 'somewhat urgent' (green) or even not urgent' (blue) the patient will have to wait in the waiting room until his turn, which will only occur when there are no more seriously ill patients to be treated.

N.º	Colour	Situation	Target time (minutes)
1	Red	Emergent	0
2	Orange	Very urgent	10
3	Yellow	Urgent	60
4	Green	Somewhat urgent	120
5	Blue	Not urgent	240

Table 1 — Basic representation of waiting queue system

2.2 Usual measures to characterize a queuing system

To model a queuing system it is crucial to characterize the arrival of the customers to the system. The arrival rate is the number of customers who, on average, arrives to the system per unit of time and is usually denoted by λ . Moreover, by computing the inverse of λ ($1/\lambda$) it is obtained the average inter-arrival time.

In what concerns to the server, it is important to know the time it takes to provide that service. The service time is the period elapsed since the service was requested until it is provided [11]. The average service rate is measured by the number of users served per unit of time and usually is denoted by μ . On the other hand, the inverse of this rate ($1/\mu$) is the average service time.

The server utilization rate, denoted by ρ , is the ratio between the average arrival rate of customers and the average service rate from the server ($\rho = \lambda/\mu$).

It is central to know the specified characteristics for computing the performance measures in a steady state, such as the average number of customers waiting in the system, the average time a customer waits in the system, the probability of having n customers in the system ($n = 0, 1, \dots$), among others [11]. The system is considered to be in a steady state when the probability distributions that characterize the system remain the same over time, i.e., the system remains described by the same distributions (a crucial condition to enable the characterization of the system).

2.3 Queue models

Kendall's notation is used to describe many models of queuing systems, where each queuing system is described by six characteristics:

- Distribution of the inter-arrival times: distribution of the time interval between consecutive arrivals;
- Distribution of service times: characterizes the length of service time;
- Number of servers in parallel;
- System capacity: maximum number of customers allowed in the system (omitted when it is infinite);
- Population size (omitted when it is infinite or, in practice, the threshold does not change the behavior of the line);
- Queue discipline (omitted when is First Come, First Served – FCFS).

Most analytical queuing models assume that the arrivals follow a Poisson distribution and a service time is characterized by an exponential distribution [23]. Moreover, the queuing systems usually fulfil the following characteristics:

- Poisson distribution for arrivals, with λ representing the average rate of arrivals;
- Exponential distribution for the service time, with μ representing the average rate of service;
- Queue discipline: FCFS;
- All arrivals wait in line to be served;
- Possibility of infinite queue length.

2.3.1 Model $M/M/s$

In this model, it is assumed that the time intervals between consecutive arrivals and the service times are independent and identically distributed (i.i.d.) with an exponential distribution (M) and there are s multiple servers, which provide independent services of each other. Figure 2 schematically depicts this model.

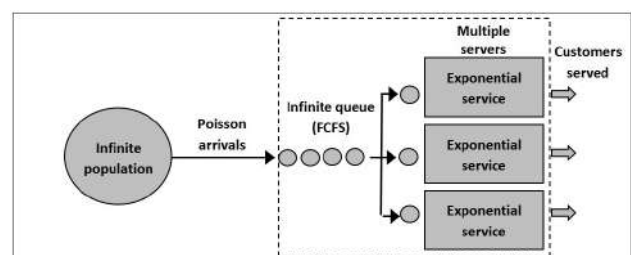


Fig. 2 — Model $M/M/S$

2.4 Queue Network

In many real situations, there is a system with multiple phases, such as shown in Figure 3. This translates the case of a traditional hospital emergency service, where a patient must go through a sequence of queues, eventually following a specific order.

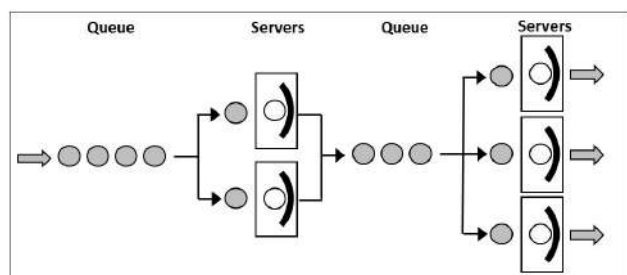



Fig. 3 — Multiple servers, multiple phases

Thus, in this case study, at the emergency service there will be a queuing system for recording the initial admission, in which the output (the departure time) will be the input (arrival time) of the second queue – the triage. In turn, the output of the triage system will be the input of the third queue – the appointment. Therefore, there is a service that encompasses several tasks. Each task returns a queue, so, consequently, this is a network system of queues. It is on this basis that the system was modeled, as explained in the next section.

3 Methodology

The main goal of this research was to develop a simulation program that generates a reliable characterization of the service operations presenting a similar behavior with the real database.

3.1 Simulation

The simulation program was developed in the  software [12, 27]. It intends to generate data as closely as possible to the real database. With this propose, the parameters corresponding to the average arrival rates, service rates, and average number of servers in each stage of the queuing system were defined. Whereas the system under study contains multiple servers with multiple phases (Figure 3), and taking into account the information provided by the hospital, it was implemented a queuing system with three phases: admission (phase 1), triage (phase 2) and appointment (phase 3). Furthermore, there were considered two servers in the admission phase, one server in triage system and four servers for the appointment phase. At all stages the queuing system is a single queue with FCFS discipline except the line for appointments, since, after the triage, the priorities are set through the Manchester system classification. The overall system is shown in Figure 4.

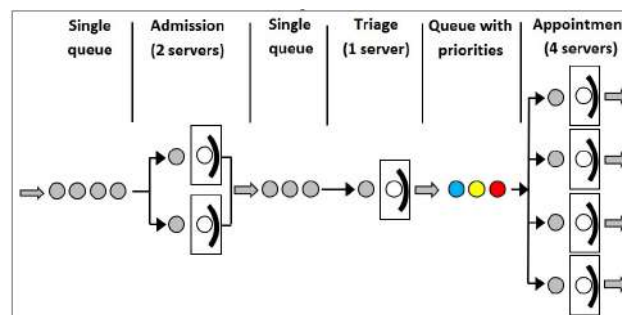


Fig. 4 — General queue system in study

The variables and parameters used in the program simulation were determined taking into account the values defined in the database. These values are shown in Table 2, where the arrival and service rates correspond to amounts per hour. Some of these values were estimated using the database information. For example, the arrival rate of patients at admission was computed by dividing the total number of records from the database by the number of hours of the year, i.e., the average number of patients that arrive at admission per hour. The rate of admission on a service server was obtained by computing the average service time length at admission and the result was 6.03 minutes. Then, one hour is divided by the average ($60/6.03 \approx 10$) obtaining the number of patients served per hour. The probability of each colour (classification in the triage) was estimate by the corresponding proportion in the database. Nevertheless, it was not possible to estimate all the parameters due to lack of sufficient information in the database. Therefore, the estimates of these parameters were obtained by trial in the simulation. There were applied different values for these parameters and then the values that generate more similar data (with the same statistical distribution) to the real data were selected. Thus, different values were tested at different simulations and the closest to the real values were selected.

Phase	Description	Value
1	Arrival rate of patients at admission	15
1	Rate of admission on a service server	10
1	Number of servers on admission	2
2	Rate of service of a triage server	21
2	Number of servers in triage	1
2	Probability of red colour on triage	.00145
2	Probability of orange colour on triage	.05984
2	Probability of yellow colour on triage	.52472
2	Probability of green colour on triage	.41081
2	Probability of blue colour on triage	.00318
3	Average service in a appoint. server	4
3	Number of servers in appointments	4

Table 2 — Some parameters of the simulation

The simulation of this research used random numbers to generate a matrix T with 8 columns, where each row corresponds to the data of each patient. Thus, the meaning of each column of the matrix T is:

- Column 1: Arrival time at hospital;
- Column 2: Admission start time;
- Column 3: End of the admission time;
- Column 4: Start time of triage;
- Column 5: End of the triage time;
- Column 6: Triage results;
- Column 7: Check-in time of the appointment;
- Column 8: Appointment departure time.

An example of a T matrix generated by one given simulation is partially shown in Figure 5. The example illustrates data for 10 patients, sorted by the arrival time to the hospital.

> T	[,1]	[,2]	[,3]	[,4]	[,5]	[,6]	[,7]	[,8]
[141,]	205.5305	206.6931	207.5058	207.5058	207.5334	4	207.7062	209.4643
[142,]	206.3429	206.7707	207.2645	207.2645	207.6211	3	207.6782	209.3311
[143,]	206.4176	207.2645	207.7954	207.7954	208.6556	3	208.6556	209.4316
[144,]	207.1583	207.5058	207.9745	207.9745	208.1252	4	208.2681	210.3923
[145,]	207.4389	207.7954	208.5910	208.5910	209.3673	3	209.4316	209.9548
[146,]	207.8972	207.9745	208.8892	208.8892	208.9786	4	209.4643	211.9667
[147,]	208.0778	208.5910	208.9532	208.9786	209.0377	2	209.3311	210.3938
[148,]	208.2460	208.8892	209.1143	209.1143	211.1090	4	211.1090	212.3957
[149,]	208.9959	208.9959	209.8463	210.0085	210.4603	4	210.4603	210.4691
[150,]	209.1371	209.1371	209.5067	209.5067	210.0085	3	210.0085	210.6588

Fig. 5 — T partial matrix simulated by software

Analyzing the matrix on the previous figure and since the generated numbers represent time (e.g., minutes) it can be seen that, for instance, the patient number 147 arrives at the hospital at 208.0778 minutes (column 1); he is in a waiting queue until being served in the initial admission, at 208.5910 minutes (column 2). The patient finishes the admission at 208.9532 minutes (column 3) and waits in the line until being served in the triage at 208.9786 minutes (column 4). Then, he ends the triage at minute 209.0377 (column 5) with a triage result of 2 (column 6), which corresponds to orange in the Manchester triage system. After the triage and once being a while in the queue, the patient begins the doctor appointment at minute 209.3311 (column 7) and leaves the appointment at 210.3938 minutes (column 8). It should be emphasized that, despite this patient have completed the triage classification later than the previous patient (row 146), he enters ahead in the appointment since he was rated as more urgent in the triage. In another example, it can be seen that the patient number 150 exits the triage at minute 210.0085 (column 5) and enters in the doctor's appointment at exactly the same moment (column 7). This illustrates that there was no queue between the triage and the appointment and a server was available.

3.2 Database

The database provided by the HSA was adapted. Data from patients who had missing values or errors in one of the measurements (e.g., a subsequent stage with an associated time prior to the time of a previous stage) were eliminated (less than 5% of the initial database). Thus, the database remained with 87173 observations, each with the following information (variables):

- Birth date;
- Gender;
- Admission date and time (arrival at the initial registration);
- Triage date and time (arrival at the triage);
- Manchester (symptoms);
- Priority (defined by Manchester triage);
- Type of medical specialty required for patient care;
- Observation date and time (arrival at doctor's appointment);
- Release date and time (hospital discharge);
- Destination (hospitalization, medical family, among others).

As previously stated, the system must be stable to develop a suitable model. Thus, the database had to be reduced to a period in which the behavior of the system was homogeneous. Figures 6 and 7 represent the complete database behavior.

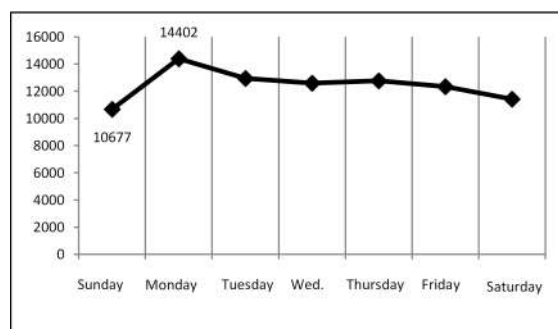


Fig. 6 — Number of Total patients by day of the week

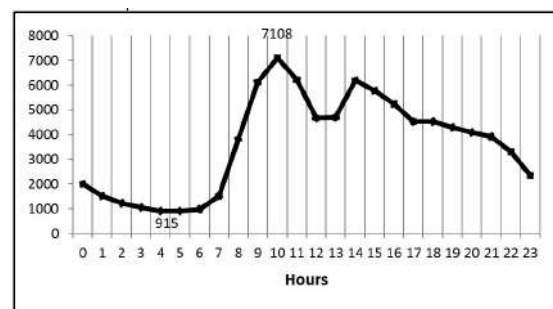


Fig. 7 — Number of Total patients by hour

Hence, considering the above graphs (and other similar comparative analysis, such as the evolution during the year of the number of patients per day and at each time interval, the number of patients per month, among others), the data selected correspond to the records of Wednesdays and Thursdays between 2:30 p.m. and 4:30 p.m., during all the year of 2014. Consequently, the applied dataset stayed with 3459 observations. In this paper, the analysis performed is restricted to these periods. However, the same methodology can be applied to other length of time as long as the period under review is stable.

3.3 Comparison of Distributions

In order to analyze the results and draw conclusions from the data provided by the simulation, it is crucial that statistical distributions from both simulation and real database match. Therefore, it was necessary to compare the two datasets with the expectation that they would be characterized by the same distributions.

It must be noted that the original database does not have all the needed values. Instead of the 7 times planned for the T matrix, as previously explained, it only has the arrival times to the initial admission, triage and appointment whereas the output times of each service are not in the dataset. Thus, we have focused on these three values. Nevertheless, if all the necessary information was available it would certainly be easier to model the system and further the estimates would be more reliable.

As a common procedure in queue theory, all the simulations performed in this study assumed an exponential distribution in all the phases of the system. Considering this assumption, the best value for each parameter was searched.

Initially, we compared the D_{ha} variable (difference between the admission time of one patient and the admission time of the previous patient, i.e. the time between two consecutive arrivals) from the real database with the same variable computed from the dataset generated by simulation (using column 2 of the T matrix). Nonparametric tests were used to compare the unknown distributions of the two independent datasets. This kind of tests only compares the observations of the two sets of data rather than specifying conditions for the distribution or even for the parameters. In this case, the appropriate test is the Kolmogorov-Smirnov test [2, 13, 30] considering as hypotheses to test:

- H_0 : the two datasets are drawn from the same distribution;
- H_1 : the two datasets are not drawn from the same distribution.

The Kolmogorov-Smirnov test for two datasets analyzes the maximum distance, D , between the two empirical

distribution functions. In Figure 8 these two distributions functions are plotted. As shown, the distance D is not significant. Therefore, it was assumed that the two datasets can be drawn from the same population. Nonetheless, the p -value obtained in the test was lower than 2.2×10^{-16} , which would lead us to reject the null hypothesis. Though, analyzing Figure 8, it may be seen that the real data were discretized (the recorded values are rounded), which does not happen in the simulated values. This discretization explains the result of the Kolmogorov-Smirnov test.

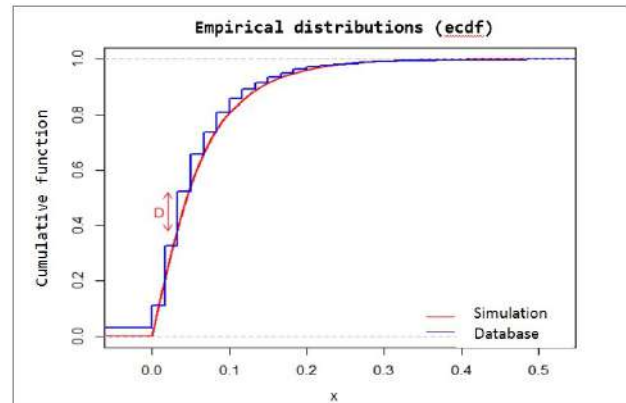


Fig. 8 — Comparison between column 2 from simulation with D_{ha} variable from database

On the other hand, considering the two sets of data, some measures of this variable (in hours) were compared (minimum, maximum, mean, median, quartiles and standard deviation – sd). The achieved results are similar (Figure 9) which supports the perception that the two datasets can follow the same distribution.

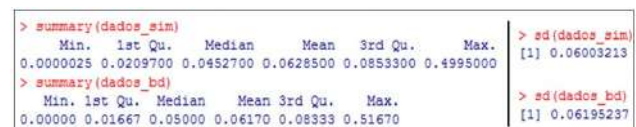


Fig. 9 — Comparison of measures for the two datasets

Another comparison of the two distributions can be performed by the quantile-quantile plot (QQ-Plot) chart [19]. This chart is applied to analyse the quantile distribution of two datasets. This chart plots the quantiles of the two datasets in the plan (simulated data and real data). If the points are aligned in a straight slope 1 ($x = y$), then the distributions of the two datasets may be considered equal. Thus, representing the two datasets, we obtain the graph of Figure 10. The majority of the points are in the line $x = y$ or are very close to it. The obtained results reinforce the idea that there is not a significant difference between the two distributions.

Another possible test to compare distributions of two datasets is the Chi-Square test [22, 25]. This test groups the observations into classes (disjoint intervals) and then compares the frequencies of these intervals between the two databases (the real and the simulated datasets). The

test returned a p -value equal to 0.4601, and therefore the null hypothesis is not rejected. Hence, considering the initial hypotheses, there is no statistical evidence that the two datasets are not drawn from the same distribution.

In conclusion, the above results show that the variable D_{ha} from the two datasets (from the real database and from the simulated database) seems to follow the same distribution, at least approximately. The same procedures were applied to compare other variables in different phases of the system, concluding that all of them appear to follow, at least approximately, the same distribution in the real and in the simulated datasets.

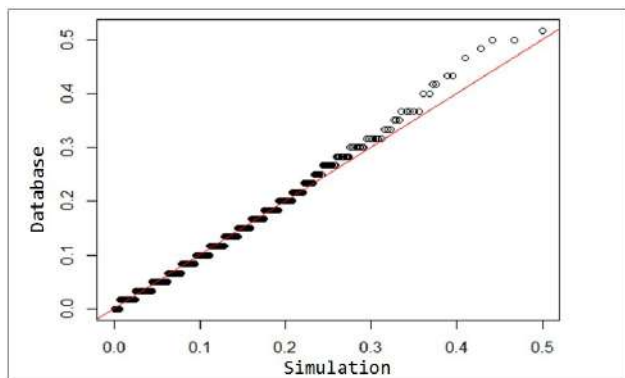


Fig. 10 — QQ-Plot between the two datasets distribution

4 Results

A sensitivity analysis was carried out, creating several scenarios by changing the values of various model's parameters. Accordingly, several simulations were performed in order to test possible benefits that may contribute to the improvement of the system efficiency. The stability of the model was also tested and both the results and the respective analyzes are presented. The results were based on the following variables:

- *tea*: average waiting time until patients begin registration on the initial admission (column 2 - column 1).
- *t_{sa}*: average time that patients are on admission, therefore, the average service admission time (column 3 - column 2).
- *t_{et}*: average waiting time since leaving admission until the start of the triage (column 4 - column 3).
- *t_{st}*: average time that patients are in the triage, i.e., the average triage service time (column 5 - column 4).
- *t_{ec}*: average waiting time since leaving the triage until starting the appointment (column 7 - column 5).
- *t_{sc}*: average time each patient is in the doctor's appointment, therefore, the average appointment service time (column 8 - Column 7).

The variables are distributed through the overall system as shown in Figure 11.

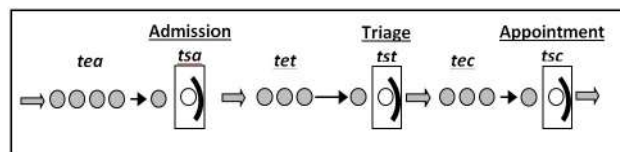


Fig. 11 — Variables analysis in the model

4.1 Changing the number of servers

By changing the number of servers at admission (value of the parameter ns) and keeping the other parameters with the same values as those defined in Table 2, were achieved the results (in hours) shown in Figure 12.

```
> tabela_ns
      tea      tsa      tet      tst      tec      tsc
ns=1 1.731903e+02 0.10139013 0.0443828 0.04764772 0.05135144 0.2494270
ns=2 1.161184e-01 0.09976613 0.1076443 0.04692426 0.71581846 0.2490607
ns=3 1.484662e-02 0.09970685 0.1137033 0.04780375 0.73548688 0.2504978
ns=4 2.557755e-03 0.09929135 0.1236386 0.04765309 0.94214117 0.2500997
```

Fig. 12 — Changes in ns (number of servers at admission)

Hence, the changing in the ns parameter value has, above all, influence on the *tea* variable (it is in the first column that there are significant differences). For $ns = 1$ oscillations can also be found in *t_{et}* and *t_{ec}* variables comparing with other values of ns . Once there is only 1 server on admission, the waiting times until the admission are high. Consequently, patients arrive to the other services more apart from each other (with longer intervals between arrivals) and do not find more queues in the system. The waiting times to get into the triage and the appointment services are then reduced (*t_{et}* and *t_{ec}* variables). The slight fluctuations in the remaining variables are due to the generation of different random numbers each time a simulation is performed. The results for each ns value are obtained through different simulations. Accordingly, it seems that the system is quite less efficient if only one server is at admission, since the waiting time in all the process is much greater than in the other simulations. On the other hand, from two servers the system seems to be acceptable. Hence, with more servers there is, as expected, a decrease in the waiting time for the admission service. However, the difference is increasingly small. Initially, the system was defined with two servers at admission which appears to be a reasonable value for this parameter, considering the inherent costs of increasing servers.

With the purpose of monitoring the response of the model to changes in several parameters, a sensitivity analysis was performed. Variations in the number of servers of the three system phases were tested to assess their impact on the efficiency of the emergency service. Therefore, further simulations were made, changing the number of servers in the triage (n_{st} parameter), then the number of servers in the appointment (n_{sc} parameter)

and keeping the other parameters on the same previously defined values (*ceteris paribus* analysis). The results showed that it would be useful to increase the number of servers in the triage to three, or at least to two (it was initially set to one). The increased number of servers in the triage led to a large decrease in the waiting time, making the system much more efficient. Regarding the number of servers in the appointment, it was found that from 6 servers the system seems reasonable, but it is with 8 servers that the system presents a better performance. With these number of servers, matrix T shows that the majority of the entry times to the appointment are equal to the triage times, meaning that the patients practically find no queue to go from the triage to the appointment. Thus, it would be advantageous to increase this number to eight (initially it was set to four). However, this increase in efficiency requires a significant increase in cost, which leads to the assumption that using six servers (much more efficient than four) may be the most suitable option. Furthermore, the use of more than eight servers apparently does not improve efficiency.

Assuming these new values for the number of servers, the average of the patient's total stay time in the hospital was computed. In other words, the average time since the patient enters the hospital (column 1 of the simulation matrix) until he leaves from the doctor's appointment (column 8 of the simulation matrix) was compared with different cases, from the initial situation ($ns = 2$, $nst = 1$, $nsc = 4$) to the identified efficient case ($ns = 2$, $nst = 3$, $nsc = 8$). Additionally, some intermediate cases were also analyzed, where nst was ranged from 1 to 3, while nsc ranged from 4 to 8. As expected, the stay time average decreases significantly with the increment of nst from 1 to 2 as well as with the increase of nsc from 4 to 6. On the other hand, the impact of changing nst from 2 to 3 servers or nsc from 6 to 8 servers is quite lower (Figure 13). Decision makers should analyze the trade-off between raising servers, which lead to a reduction of patient's stay time, and the inherent costs of that decision.

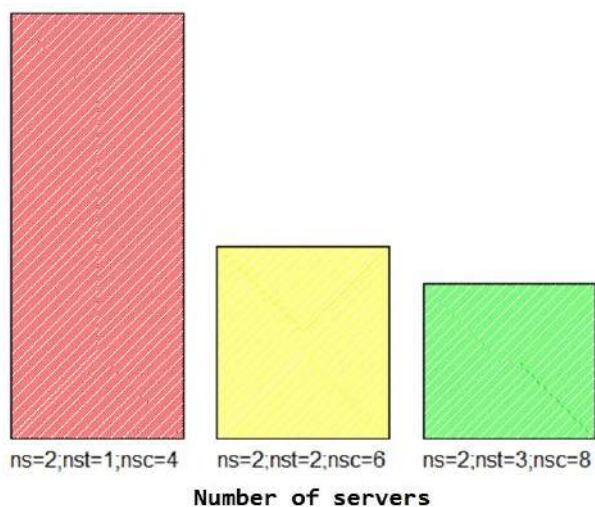


Fig. 13 — Stay time in hospital

4.2 Results from triage efficiency

After computing the average waiting time for the doctor's appointment, it was established that the greater the urgency of the patient, the shorter is the waiting time (as this is the goal of triage). The average waiting time (in hours) reduces sharply when considering the effective parameters as shown in Figure 14. No queue is reached by the users classified with the red colour, confirming the efficiency of the system with these new parameters. The red colour indicates the greatest urgency and the blue the not urgent cases.

```
> da triagem_para_consulta
Initial param.  Red   Orange   Yellow   Green   Blue
Waiting time   0.04090616 0.05636194 0.1223546 1.884396 8.742427
Efficient param. Red   Orange   Yellow   Green   Blue
Waiting time   0 0.001294909 0.001369415 0.002737718 0.007303118
```

Fig. 14 — Waiting times after triage

4.3 Model stability

Simulation is an artificial process, which imitates the behavior of a random phenomenon. Moreover, the greater the number of replicates performed in the simulation, the higher the reliability of the results. Hence, in order to obtain stable results, at least 15000 patients were used in all simulations.


Nevertheless, in order to assess the stability of the model with the applied number of patients, 100 sequences of some simulations were performed. The access to these sequences allows to analyse the variability of the main results. It was analysed three variables that characterize the entire model: the time between two consecutive arrivals admissions; the difference between the times of column 4 and column 2 of the matrix T , and the difference between the times of column 7 and column 4 of the matrix T . Moreover, in each sequence the mean, the median and the standard deviation of each of these three variables were computed. Thus, we can compare the variability of the obtained results in 100 independent simulations. Indeed, in all those measures, the interquartile range (difference between the third and the first quartiles) of the achieved values in the 100 simulations is small and the distances between the minimum and the maximum are not significant. Only the mean and standard deviation of the latter variable take some more distant values, that is, in some simulations the obtained values were further apart (the maximum value is farthest from the other values in the 100 simulations). However, as we are looking at a system, the last variable accumulates the variability that exists in the previous phases. Thus, it is expected to have more variability. Likewise, it also happens in the actual data of hospitals where there are some periods in which the number of patients exceeds the predicted values and, therefore, the waiting time increases significantly.

Nevertheless, these characteristics show that there is no significant variability of the simulated data, indicating

that the simulation system is stable with the applied number of replicas.

The stability of a simulation must be highlighted when increasing the number of sequences implemented. This is instrumental to obtain a more accurate description of the characteristics of the system under study, emphasizing the role of the simulation in the analysis of the results.

5 Conclusion and future work

An emergency service that is concerned with the patients' waiting times should take actions to improve them, if these times are unreasonable. This idea was the basis of this study. Thus, a simulation model was developed through the  software to study the efficiency of an emergency department and its benefits to patients. Hence, several scenarios were tested in order to find a solution that satisfies both the patients and the decision-makers. The big advantage of this approach lies in the fact that in a short time the model can simulate even years of operation of a typical system, generating a series of statistical observations of the system performance over that period [23].

Hence, the main goal of this simulation study was to portray, as reliably as possible, the queues system of the HSA emergencies. For this purpose, it was required to identify the underlying distributions as well as to estimate the required parameters. Thus, it was essential to look for the distributions and parameters that best describe the system under study. In order to match statistically the simulated data with the real data, in the sense that both are described by the same distributions, all the provided data were taken into consideration in the simulation model configuration. However, the identification or modeling of the distribution of each service time was not possible because the required data were not provided by HSA (as previously stated, the HSA database does not include all the needed information). This is a clear constraint in the current study, since if all the information was available then it would be possible to apply nonparametric methodologies to estimate the distribution underlying each specific phase. Consequently, the usual distributions were applied and, under this condition, the associated parameters were estimated.

In this study there were not considered the economic factors that are intrinsic to the efficiency of a system, for instance, the ones supported when the number of servers is increased. Rather, an attempt was made to find the best performance for the queue system model regardless of the involved costs. Therefore, taking into account the associated costs with the different configurations of the system, it is not possible to state that the efficient solution ($n_s = 2$, $n_{st} = 3$, $n_{sc} = 8$) is the optimal one, since a whole set of other factors that influence decision-making was not taken into consideration. Nevertheless, although

the inherent costs were not included in the model, they were intuitively considered. Comparing the three cases illustrated in Figure 13, it may be realized that the increase cost from changing of the first to the second position is the same carried out when changing from the second to the third position. However, the gain in efficiency is much more significant in the first modification. This difference in the impact on the efficiency of the system supports the idea that the first change should be implemented. On the other hand, the latter should be subject to a deeper analysis taking into account all the operational costs.

This research study aimed at providing insights about an efficient management of a queue system, in order to improve waiting times as well as service capacity in Hospital emergencies. However, the effective management of a service capacity must deal with complexities such as the compromise between flexibility and the quality of assistance, types of patients, the intervals between various arrivals, unpredictable situations and, often, the different perspectives of managers, doctors, nurses and patients. On the other hand, it must be emphasized that this study was restricted to a specific schedule and, therefore, to obtain a complete research, a similar analysis to the adjacent schedules is required.

All these factors are challenges that affect the ability of hospital managers to control costs and simultaneously to improve the quality of health care delivery. To address these challenges, managers must have access to data and performance measures of the system, in order to use this information for decision making. Furthermore, simulation allows evaluating the impact of changes in the system, thereby obtaining information that cannot be achieved by experimentation or intuitively. Thus, the queuing systems analysis and its simulation modeling are one of the most practical and effective tools for understanding these systems. This approach highlighted that it should be addressed in the decision making process when dealing with critical resources management of the medical community.

Regarding the case study, it would be important to improve the data contained in the hospital's database in order to overcome the previously mentioned limitations. Thus, the registration of the time data of each service is crucial to allow the estimation of the underlying distributions of each of these times (at least approximately) through the use of nonparametric statistics methodologies. In fact, the waiting times or service times available on the HSA database included more than one phase of the system, corresponding to the sum of two or three phases (usually at least one waiting time in a queue and a service time). Therefore, the observed distributions correspond to the sum of two or three distributions and, consequently, the application of nonparametric methodologies are not feasible (at least in a straightforward way). Other information that is not in the dataset is the arrival time to the hospital of each user. Hence, HSA should implement some mechanical or computer devices to collect automa-

tically all the required data. This would be a definitive step towards the implementation of an information system in order to allow a continuous critical analysis of the system performance.

Finally, one possible forthcoming research to enhance this approach is to develop a similar study in other hospital services or in other hospital units. It would also be interesting to optimize the simulation model, creating an application that would allow to quickly changing the system parameters and measuring the impact on service performance. This would turn quite easy to observe the consequences in the system when, for instance, the number of doctors change or there is a raise in the patient arrivals.


Acknowledgements



This study was developed by Mário Carvalho as part of the master's degree dissertation [4] in Healthcare Information Systems Management (ESTG-IPLeia and FMUP) under the supervision of Rui Santos and Liliana Ferreira.

This study was partially supported by Fundação para a Ciência e a Tecnologia under the projects UID/MAT/04561/2013 and UID/MAT/00006/2013.

The authors thank the Hospital de Santo André of Leiria for giving access to their 2014 emergency services data. Without this information it would be impossible to carry out this study.

Referências

- [1] M. Alavi-Moghaddam, R. Forouzanfar, Sh. Alamdari, A. Shahrami, H. Kariman, A. Amini, Sh. Pourbabae, A. Shirvani, Application of Queuing Analytic Theory to Decrease Waiting Times in Emergency Department: Does it Make Sense? *Arch Trauma Res.* 1 (2012) 101-7.
- [2] T. Bolen, D. Mulugeta, J. Greenfield, L. Conkey, *An Investigation of the Kolmogorov-Smirnov Two Sample Test using SAS*, Cardinal Health, 2014.
- [3] J.C. Carvalho, T. Ramos, *Logística na Saúde*, Sílabo Edition, 2013.
- [4] M. Carvalho, *Caracterização de uma Fila de Espera de um Serviço Hospitalar – Um Estudo de Caso*. Master thesis, Polytechnic Institute of Leiria, 2015.
- [5] De Bruin, M. Arnoud, A.C. Van Rossum, M.C. Visser, G.M. Koole, Modeling the emergency cardiac inpatient flow: an application of queuing theory, *Health Care Manage Sci* 10 (2007) 125-137.
- [6] A. Elalouf, G. Wachtel, An alternative scheduling approach for improving patient-flow in emergency departments, *Operations Research for Health Care* 7 (2015) 94-102.
- [7] L.V. Green, *Using Operations Research to Reduce Delays for Healthcare*. Tutorials in Operation Research, INFORMS, 2008.
- [8] D. Gross, J.F. Shortle, J.M. Thompson, C.M. Harris, *Fundamentals of Queueing Theory* (4th ed.). John Wiley & Sons, 2008.
- [9] Grupo Português de Triagem. Available in <http://www.grupoportuguestriagem.pt>.
- [10] R.W. Hall (Ed.), Patient Flow: Reducing Delay in Healthcare Delivery. *International Series in Operations Research & Management Science* 91, Springer, 2006.
- [11] F.S. Hillier, G.J. Lieberman, *Introduction to Operations Research* (8th ed.), McGraw Hill, New York, 2005.
- [12] O. Jones, R. Maillardet, A. Robinson, *Introduction to Scientific Programming and Simulation Using* . CRC Press, Taylor & Francis Group, 2009.
- [13] A. Justel, D. Peña, R. Zamar, A multivariate Kolmogorov-Smirnov test of goodness of fit. *Statistics & Probability Letters* 35 (1997) 251-259.
- [14] D. Lin D, J. Patrick, F. Labeau, Estimating the waiting time of multi-priority emergency patients with downstream blocking. *Health Care Management Science* (2013) 1-12.
- [15] Z. Liu, E. Cabrera, M. Taboada, F. Epelde, D. Rexachs, E. Luque, Quantitative Evaluation of Decision Effects in the Management of Emergency Department Problems, *Procedia Computer Science* 51 (2015) 433-442.
- [16] C. Lobo, *Otimização do Atendimento Permanente de Adultos do Hospital CUF Porto*. Porto University, 2013.
- [17] V. Macedo, *Especificação do Fluxo Cirúrgico num Serviço de Ortopédia com Base na Simulação*. Porto University, 2012.
- [18] L. Mayhew, D. Smith, Using queueing theory to analyse the government 4h completion time target in Accident and Emergency departments. *Health Care Manage Sci* 11 (2008) 11-21.
- [19] NIST/SEMATECH. *e-Handbook of Statistical Methods*, 2015. Available in <http://www.itl.nist.gov/div898/handbook/eda/section3/qplot.htm>.
- [20] Y.A. Ozcan, *Quantitative Methods in Health Care Management: Techniques and Applications*, 2nd Edition, Wiley, 2009.
- [21] C. Pereira, *Uma Introdução às Filas de Espera*. Madeira University, 2009.

- [22]  Documentation, *Pearson's Chi-squared Test for Count Data*. Available in <https://stat.ethz.ch/R-manual/R-patched/library/stats/html/chisq.test.html>.
- [23] A.K. Sharma, R. Kumar, G.K. Sharma, Queueing Theory Approach with Queueing Model: A Study, *International Journal of Engineering Science Invention* 2 (2013) 1-11.
- [24] D. Sinreich, Y. Marmor, Ways to reduce patient turnaround time and improve service quality in emergency departments, *J Health Organ Manag* 19 (2005) 88-105.
- [25] J.R. Taylor, *An introduction to error analysis*. California: University Science Books, 1997.
- [26] T. Veloso, *Gestão de Filas de Espera no Serviço de Urgência*. Minho University, 2011.
- [27] W.N. Venables, D.M. Smith, and the  Core Team. *An Introduction to R*, 2015. Available in <http://cran.r-project.org/doc/manuals/R-intro.pdf>.
- [28] J. Vile, *Time-Dependent Stochastic Modelling for Predicting Demand and Scheduling of Emergency Medical Services*. Cardiff University, 2013.
- [29] J. Wang, K. Li, K. Tussey, K. Ross, Reducing Length of Stay in Emergency Department: A Simulation Study at a Community Hospital. *IEEE Transactions on Systems, Man, and Cybernetics, Part A*. 42 (2012) 1314-1322.
- [30] J. William, *Practical Nonparametric Statistics*. John Wiley & Sons, New York, 1971.



Searching for the Fourth Dimension, Salvador Dali (1979)

Quaternion Rotations and its applications

by NELSON MARTINS-FERREIRA

Centre for Rapid and Sustainable Product Development
School of Technology and Management
Polytechnic Institute of Leiria, Portugal
martins.ferreira@ipleiria.pt

Abstract In this short article we recall the basic properties of the quaternion algebra and use the fact that quaternion multiplication can be used as an efficient tool to work with rotations on the 3D-space. We give two practical examples of application and detail their implementation in Matlab and Octave. The first case is useful to perform rotations of a planar curve defined on the complex plane which is identified with the yz -plane in the 3-space. Then the rotation moves the x -direction to the direction orthogonal to the desired resulting plane containing the planar curve. This has several applications on 3D-printing, for example it can be used to generate a surface by placing successive planar curves (interpreted as crossed sections) along a structural curve on the 3D-space. The second case is useful in rotating a planar face to meet the orthogonal direction of an adjacent planar face. This can be used to compute geodesic trajectories on a surface patched by arbitrary planar faces.

Keywords: Quaternion algebra, rotations on the 3-space, rotation of a planar face to meet the orthogonal direction of another planar face, rotation of a planar curve on the complex plane.

1 Introduction

The main purpose of this paper is to illustrate the power and apparent simplicity of quaternion multiplication to work with rotations in the 3D-space. We give the basic details and main properties of the quaternion algebra and illustrate them with two examples of application. The first example is to rotate the space so that the x -axis moves to a new position, given as input, in spherical coordinates. This example is important because it can be used for placing a planar curve, which is initially considered as lying in the yz -axis and then rotated so that its normal vector is parallel to the specified one. See [4] for a concrete example. The same procedure can also be used to generate a surface, along a structural curve in the 3D-space, with variable cross-sections. This has important applications on 3D-printing and related topics. Another example is to rotate a face of a polyhedra, along a specified edge, so that it becomes parallel to its adjacent face along the specified edge. This can be applied, for instance, in computing geodesic paths on surfaces that are patched by planar faces with arbitrary number of sides.

For a short note on the subject see e.g. [1]. Further references are, e.g. [3, 2].

2 The quaternion algebra

The quaternion algebra \mathbb{H} is a set $\mathbb{H} = \mathbb{R} \times \mathbb{R}^3$, together with two constants, $0 = (0, (0, 0, 0))$ and $1 = (1, (0, 0, 0))$, and two binary operations: addition and multiplication. In order to simplify notation, and following the intuition on complex numbers, we will write an element $a \in \mathbb{H}$,

that is $a = (a_0, a_1) = (a_0, (a_{11}, a_{12}, a_{13}))$ as a sum

$$a = a_0 + a_{11}i + a_{12}j + a_{13}k$$

where i, j, k represent the vectors in the canonical basis of \mathbb{R}^3 . See Figure 1.

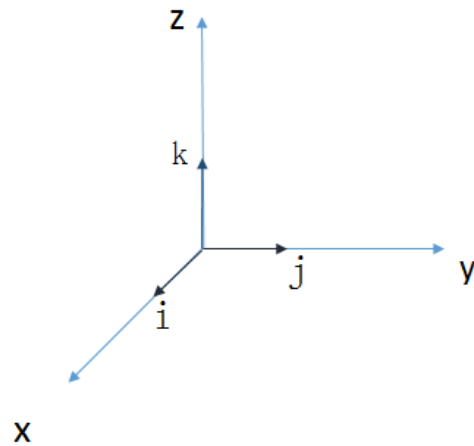


Fig. 1 — Vectors i, j, k representing the canonical basis of the 3-space.

Addition is the usual addition in $\mathbb{R}^4 \cong \mathbb{R} \times \mathbb{R}^3$ while multiplication is determined by the interaction between i, j, k as follows

$$i^2 = j^2 = k^2 = -1 \tag{1}$$

$$\begin{aligned} ij &= k, & ji &= -k \\ ki &= j, & ik &= -j \\ jk &= i, & kj &= -i. \end{aligned} \tag{2}$$

The formulas in (2) are obtained by the usual cross product of vectors in space, following the direction of the right hand rule. A possible interpretation of the fact that $i^2 = j^2 = k^2 = -1$ is that the cross product of two parallel vectors always vanishes, and hence its vector part is null, however it remembers some traces of the inner product.

Note that the identities $i^2 = j^2 = k^2 = ijk = -1$ also determine all the possible interactions of i, j, k and hence the multiplicative structure of the quaternion algebra.

The general formula for the multiplication of two quaternions may thus be presented in the form

$$(a_0, a_1)(b_0, b_1) = (a_0b_0 - a_1 \cdot b_1, a_0b_1 + a_1b_0 + a_1 \times b_1) \quad (3)$$

where \cdot is the inner (or scalar) product of two vectors and \times is the outer (or cross) product of two vectors.

The norm of a quaternion is the usual norm when it is considered as a vector in \mathbb{R}^4 . The conjugate of $a = (a_0, a_1)$ is $\bar{a} = (a_0, -a_1)$ and the inverse of a , when $\|a\| \neq 0$, is $a^{-1} = \frac{\bar{a}}{\|a\|^2}$.

3 Quaternion rotations

The formula

$$e^{i\theta} = \cos(\theta) + i \sin(\theta)$$

is the basic fact that explains why the multiplication of complex numbers can be used to handle rotations in the plane. Indeed, if $v \in \mathbb{R}^2$, then the operation $v' = e^{i\theta}v$ has the effect of rotating the vector $v \in \mathbb{R}^2$, considered as a complex number, counter-clockwise around the origin by an angle of θ radians.

The case of 3-dimensions is more subtle and it involves one extra dimension. The formula for rotating in 3-space depends on a unit vector $u \in \mathbb{R}^3$, that is, with $\|u\| = 1$, the axis of rotation, and an angle of rotation, θ . Having this data we build the quaternion

$$q = e^{\frac{\theta}{2}u} \quad (4)$$

with $u = (u_i, u_j, u_k) \in \mathbb{R}^3$ considered as a pure quaternion $u = (0, (u_i, u_j, u_k))$.

The operation

$$v' = qvq^{-1}$$

returns v' , the result of rotating the vector v around u , counter-clockwise, by θ radians.

The exponential map e^x , defined as the series

$$\sum_{n=0}^{\infty} \frac{x^n}{n!}$$

when it is absolutely convergent, makes sense in every algebraic structure with addition and multiplication, which is the case of quaternion numbers.

It turns out that in the concrete case of quaternions the exponential map can be expressed as

$$e^a = \sum_{n=0}^{\infty} \frac{a^n}{n!} = e^{a_0} \left(\cos\|a_1\| + \frac{a_1}{\|a_1\|} \sin\|a_1\| \right),$$

with $a = (a_0, a_1) \in \mathbb{H}$.

In particular, when a is of the form $(0, \theta u)$, with $\theta \in \mathbb{R}$ and $u \in \mathbb{R}^3$ a unit vector, then

$$e^a = (\cos \theta, u \sin \theta).$$

With this simplification, given an angle $\theta \in \mathbb{R}$, and a unit vector $u \in \mathbb{R}^3$, we observe that the quaternion q , defined as in formula (4), is of the form

$$q = \left(\cos \frac{\theta}{2}, u \sin \frac{\theta}{2} \right),$$

while its inverse is simply $q^{-1} = \left(\cos \frac{\theta}{2}, -u \sin \frac{\theta}{2} \right)$.

We may thus summarize the procedure of rotating a vector $v \in \mathbb{R}^3$, by an angle θ , counter-clockwise, around the direction of the unit vector $u \in \mathbb{R}^3$, as follows:

1. define the quaternion $q = \left(\cos \frac{\theta}{2}, u \sin \frac{\theta}{2} \right)$, and observe that $q^{-1} = \left(\cos \frac{\theta}{2}, -u \sin \frac{\theta}{2} \right)$;
2. consider $v = (0, v)$ as a pure quaternion and use the quaternion multiplication to get $v' = qvq^{-1}$;
3. it follows that v' is a pure quaternion, that is, a vector in \mathbb{R}^3 ; moreover, v' , as a vector, is the result of rotating the vector v , by θ radians, counter-clockwise, around the direction of the unit vector u .

We will now study two examples of application.

4 Example of application 1

Suppose we have a curve in the complex plane and we would like to place this curve in the 3-space in such a way that its normal vector would be parallel to a given direction of the 3-space.

One way to do this is to identify the complex plane with the yz -plane of the 3D-space, whose normal is the x -axis, and then compute the rotation needed to take $x = (1, 0, 0)$ to coincide with the given direction to which we would like the planar curve to be orthogonal to.

The procedure to do that can be performed as follows.

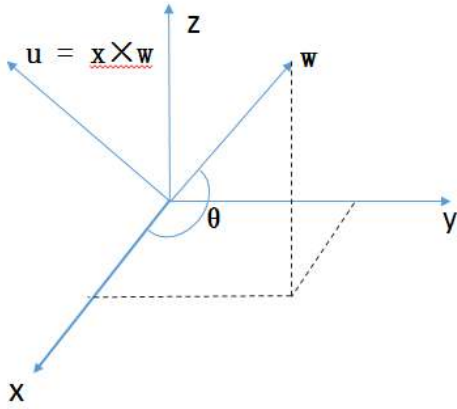


Fig. 2 — Rotating the x -axis by θ radians, counter clockwise, along the direction $u = x \times w$, has the effect of moving x to meet w .

Suppose w is the vector giving the direction to which we would like the planar curve to be orthogonal to. Then, in this case, the rotation is about the vector $u = x \times w$, the cross product between the x -axis considered as the vector $(1, 0, 0)$ and the vector w , and the angle is θ , as illustrated in Figure 2, the angle between x and w .

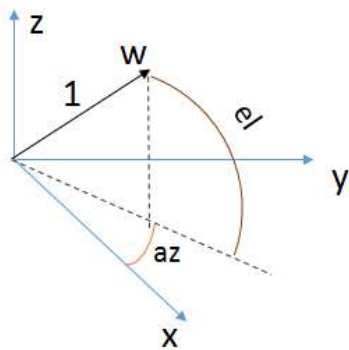


Fig. 3 — Illustration of azimuth az and elevation $e1$ for a unitary vector w

The cross product and the dot product (which can be used to determine the angle) may be computed at the same time by simply using the formula (3). Specifically, if we let $x = (0, (1, 0, 0))$ and $w = (0, \text{sph2cart}(az, e1, 1))$, where we assume that the vector w is unitary and given in spherical coordinates by defining its azimuth and elevation, as illustrated in Figure 3, we get, using the formula for quaternion multiplication,

$$\begin{aligned} xw &= (0, (1, 0, 0))(0, \text{sph2cart}(az, e1, 1)) \\ &= (-\cos(\theta), u \sin \theta) \end{aligned}$$

with θ the angle between the x -axis and the vector w , and u the unit vector whose direction is orthogonal to the x -axis and to the vector w , following the right hand rule, from the x -axis to the vector w , as illustrated in Figure 2.

We can thus extract the angle between the x -axis and w as

$$\theta = \text{acos}(-\text{real}(xw))$$

and we can extract u as

$$u = \frac{1}{\sin \theta} \text{pure}(xw).$$

This means that, by the procedure outlined in the previous section, we can define $v' = qvq^{-1}$, with $q = (\cos \frac{\theta}{2}, u \sin \frac{\theta}{2})$ and $q^{-1} = (\cos \frac{\theta}{2}, -u \sin \frac{\theta}{2})$.

The procedure is implemented into m-code, as illustrated in the Appendix of this text. It is implemented in the form of an m-function called `xgoestow` which should be read as: the direction of x goes to the direction of w .

Remark When $\theta = \text{acos}(-\text{real}(xw))$ is 0 or π , then the value of u cannot be extracted. The case $\theta = 0$ corresponds to $w = (1, 0, 0)$, while the case $\theta = \pi$ corresponds to $w = (-1, 0, 0)$. We can set $v' = v$ when $w = (1, 0, 0)$, but there is no natural choice when $w = (-1, 0, 0)$. To the application that we have in mind we have chosen to set $v' = (-v_1, v_2, v_3)$ if $v = (v_1, v_2, v_3)$.

5 Example of application 2

For the second example of application, suppose we have two faces of a polyhedra, F_1 and F_2 , and that these two faces share a common edge, as illustrated in Figure 4 for an example with square faces.

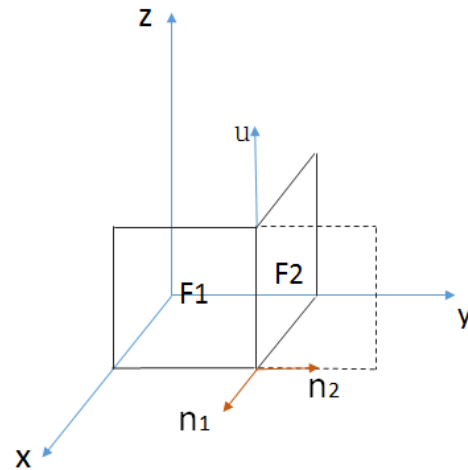


Fig. 4 — An example of two planar faces F_1 and F_2 , sharing a common edge. The vectors n_1 and n_2 are the respective normal vectors while u is the orthogonal direction to both vectors, and it is also the direction of the common edge.

Our goal is to rotate the face F_2 so that it becomes parallel to the face F_1 . This rotation should be made around the common edge, the direction of the vector u in the picture, which is the same as the direction of the vector obtained by the cross product of the two normal

vectors to each one of the two faces, $u = n_1 \times n_2$ (see Figure 4). The angle of rotation is the angle between n_1 and n_2 , respectively, the normal vectors to the faces F_1 and F_2 .

Following the same procedure as above, assuming the faces F_1, F_2 are given, we have:

1. define n_1 as the normal vector to the face F_1 and let it be a pure quaternion;
2. define n_2 is a similar way with respect to the face F_2 ;
3. let $n_{12} = n_1 n_2$ be the quaternion obtained by taking the quaternion multiplication of n_1 with n_2 ;
4. define θ as the arc whose cos is the real part of n_{12} and let u be the pure part of it, divided by $\sin(\theta)$;
5. define q as the quaternion exponential of $\frac{\theta}{2}u$, considered as a pure quaternion;
6. for each vertex v in the face F_2 perform the operation qvq^{-1}

This procedure is illustrated in the appendix.

Note that in this case, when n_1 is parallel to n_2 , we have $\theta = 0$ or $\theta = \pi$, which causes difficulties in defining u . In that case we have to *force* u to have the direction of the common face which is assumed to exist between the two faces.

6 Appendix: M-code listing

This appendix contains the M-code that implements the two examples described in the text.

6.1 Listing for the first example

If C is a vector of complex numbers, describing a planar curve on the complex plane, and if w is a unit vector on the 3-space, given in spherical coordinates (az, el) then, the instruction $V=[\text{real}(C), \text{imag}(C), \text{zeros}(\text{size}(C))]$, combined with $V=\text{xgoestow}(V, az, el)$, returns the position V of the curve C placed in the 3D-space, which is orthogonal to the direction (az, el) .

```
function V=xgoestow(V,az,el)
% V=xgoestow(V,az,el)
%
% Returns the rows of V, considered as vectors in 3D-space,
% rotated in such a way that the yz-plane is transformed
% into a plane which is orthogonal to the direction
% given by sph2cart(az,el,1), with az the azimuth and el
% the elevation in spherical coordinates.

x=[0 1 0 0]; % the x-axis considered as a pure quaternion
w=[0 sph2cart(az,el,1)]; % w, the direction orthogonal to the
% transformed yz-plane, as a pure quaternion
xw=quatmultiply(x,w);
```

Acknowledgement

We would like to acknowledge the Portuguese foundation for Science and Technology (FCT), for the funding of this research work. Project reference UID/ Multi/04044/2013.



Referências

- [1] N. Martins-Ferreira, *The quaternion algebra*, Scripta-Ingenia 4 (June) (2015) 1–2.
- [2] Conway, John H., and Derek A. Smith, *On quaternions and octonions*, Taylor & Francis (2003)
- [3] Ian R. Porteus, *Topological Geometry*, Van Nostrand Reinhold (1969)
- [4] V. Mahendra and N. Martins-Ferreira, *Movement of water molecules — a mathematical outlook*, Scripta-Ingenia 7 (December) (2016) 9–13.

```

theta=acos(-xw(1)); % the angle between x and w
u=xw(2:4); % the direction orthogonal to x and w
q=quatexp(theta/2*[0 u]); % the rotation quaternion
qinv=quatinv(q);
qrep=repmat(q,size(V,1));
qinvrep=repmat(qinv,size(V,1));
Vpure=[zeros(size(V,1),1) V];
V=quatmultiply(qrep,quatmultiply(Vpure,qinvrep));

```

6.2 Listing for the second example

```

n1=[0, normal(F1)]; %the normal vector to F1 considered as a pure quaternion
n2=[0, normal(F_2)];
n12=quatmultiply(n1,n2);
theta=acos(-n12(1));
u=n21(2:4);
q=quatexp(theta/2*[0 u]); % the rotation quaternion
qinv=quatinv(q);
qrep=repmat(q,size(F2,1));
qinvrep=repmat(qinv,size(F2,1));
F2pure=[zeros(size(F2,1),1) F2];
V=quatmultiply(qrep,quatmultiply(F2pure,qinvrep));

```

Ficha Técnica

Director: Nelson Martins Ferreira
 Proprietário: Instituto Politécnico de Leiria, anotado na ERC
 Morada: Rua General Norton de Matos; Apartado 4133; 2411-901 Leiria, Portugal
 Director Adjunto: Nuno Alves; Sub Director: Artur Mateus
 Editor: Nelson Martins Ferreira; Sede de Redação: Edifício IPL, Rua de Portugal – Zona Industrial 2430-028 – Marinha Grande, Portugal; Contacto: scripta.ingenia@ipleiria.pt
 Colaboradores e estatuto editorial: <http://cdrsp.ipleiria.pt/scriptaingenia/>